

# *Simulation of the Antenna Pattern of Arbitrarily Oriented Very Large Phase/Time-Delay Scanned Antenna Arrays with Systematic and Random Errors*

Carlos R. Ortiz, Ph.D.  
Associate Professor  
Department of Electrical Engineering  
Polytechnic University of Puerto Rico  
email: cortiz@pupr.edu

---

## **ABSTRACT**

A computer simulation to determine the field-pattern of arbitrarily oriented, very large phase/time delay scanned antennas was developed. The simulation takes into account errors present in antenna arrays. These are systematic and random errors. The systematic errors considered here are the finite quantization of the phase produced by the use of digital N-bits phase/time-delay shifters and the flexing of the array aperture due to its large size and weight. The random errors considered are those caused by variations on the amplitude and phase of the elements current, variations on the radiation pattern of the elements, missing elements (due to catastrophic failure) and variations in the location of the elements. A number of patterns were computed to validate the simulation. These included patterns of linear arrays, array panels, and arrays of panels. Experience as well as specific examples found in the literature validated the ideal patterns. The "random-error-patterns" were compared to specific trends noted in earlier studies. The behavior of the computed patterns confirmed such trends.

## **SINOPSIS**

Desarrollo de una simulación de computadoras para determinar el patrón de radiación de antenas "scanned" arbitrariamente orientadas y con un retraso grande en fase/tiempo. La simulación considera los errores presentes en arreglos de antenas. Estos errores son de naturaleza sistemática y aleatoria. Los errores sistemáticos considerados aquí son cuantización de la fase producida por el uso de "N-bits phase/time delay phase shifters" y del estiramiento de la apertura del arreglo debido a su gran tamaño y peso. Los errores aleatorios considerados son aquellos causados por las variaciones en la amplitud y fase de los elementos de corriente, variaciones en el patrón de radiación de los elementos y elementos

desaparecidos (debido a fallas catastróficas), y variaciones en la localización de los elementos. Para validar la simulación, se computó un número de patrones de casos conocidos. Estos incluyen el patrón de un arreglo lineal de elementos, paneles de arreglos lineales, y arreglos de paneles. La experiencia al igual que ejemplos específicos encontrados en la literatura validan los patrones ideales. Los "patrones-de-errores-aleatorios" se compararon contra tendencias específicas notadas en estudios previos. El comportamiento de los patrones computados confirmaron dichas tendencias.

## **I- INTRODUCTION**

The purpose of this effort was to write a simulation to compute the field of arbitrarily oriented, very large phase/time-delay scanned antenna arrays with systematic and random errors. As explained in Collin and Zucker [1], errors in antenna arrays can be divided into two categories depending on whether they are predictable (systematic) or random. Among systematic errors is the finite quantization of the phase produced by the use of digital N-bits phase/time-delay shifter. Another systematic error considered here is the flexing of the array aperture due to its large size and weight. Random errors are caused by variations on the amplitude and phase of the elements current, variations on the radiation pattern of the elements, missing elements (due to catastrophic failure) and others not considered here. Random errors may alter antenna parameters such as increasing sidelobe level, reducing power gain, lowering directivity, etc.

## **II- THEORY**

The development of the necessary equations to simulate the field pattern of arbitrarily oriented, very large planar phase/time-delay scanned antenna arrays with systematic and random errors is

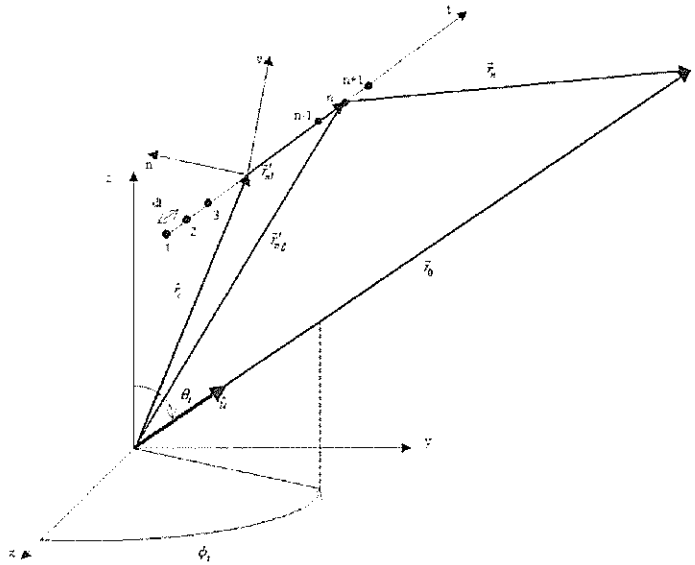


Figure 1: N-Elements Linear Array

presented in this section. Such development is based on the known principle of pattern multiplication [1].

#### A- LINEAR ARRAYS

Consider the N-elements linear array shown in Figure 1. The array axis is in the  $\hat{t}$  direction. The center of the array coincides with the origin of the t-axis and it is specified, with respect to a Cartesian (global) coordinate system, by the position vector  $\hat{r}_c$ . For an even number of elements, the elements are distributed equally on each side of the array. For an odd number of elements, the center element is located at the origin of the t-axis with an equal amount of elements on each side. The distance between any two consecutive elements is constant and it is represented by "d<sub>i</sub>". The elements are considered to be identical, with identical magnitude and progressive phase shift between consecutive elements. Such array can be referred to as a uniform array.

According to the method of pattern multiplication, the far-field pattern of an array of identical elements is equal to the product of the element pattern and the array factor of the array. The element pattern is the field of a single element computed at a reference point -usually the origin of the array. The array factor is a function of the number of elements, their geometrical arrangement, their relative magnitude and phases, and their spacing.

Thus, the transmitting field pattern of the array of Figure 1 may be written as:

$$F_N(\theta, \phi) = e^{\delta_N}(\theta, \phi) f_N(\theta, \phi) \quad (1)$$

where  $e^{\delta_N}(\theta, \phi)$  represents the element pattern with random error and can be expressed as [2]  $e_N^{\delta} = e_N (1 + \delta e_N) \kappa$ , where  $e_N$  is the non-error element pattern,  $\delta e_N$  are samples of a random variable with zero mean and variance  $\sigma_{\delta e_N}^2$ , and the factor  $\kappa$  accounts for missing elements such as those that might be caused by catastrophic failure. As in Collin and Zucker [1], it is assumed that  $\kappa$  represents the fraction of elements that remain when  $1 - \kappa$  elements have failed. On the other hand,  $f_N(\theta, \phi)$  represents the array factor. For now, we will assume isotropic elements with  $\sigma_{\delta e_N}^2 = 0.0$  and  $\kappa = 1.0$  so that  $e_N^{\delta}(\theta, \phi) = e_N(\theta, \phi) = 1.0$ . Now,  $f_N(\theta, \phi)$  becomes the entire radiation pattern. Thus,

$$F_N(\theta, \phi) = \sum_{n=1}^N I'_n e^{j\beta (\hat{u} \cdot \hat{x}_n)} \quad (2)$$

In equation (2),  $\beta = \frac{2\pi}{\lambda}$  where  $\lambda$  is the wavelength.  $I'_n$  is the excitation with random error at the  $n^{\text{th}}$  element which can be expressed as [2],

$$I'_n = (1 + \delta I_n) |I_n| e^{j(\alpha_n + \delta\alpha_n)} \quad (4)$$

where  $|I_n|$  and  $\alpha_n$  are the non-error magnitude and phase of the excitation. The  $\delta I_n$  as well as the  $\delta \alpha_n$  are samples of random variables assumed to have a normal distribution with zero mean and variance  $\sigma^2 \delta I_n$  and  $\sigma^2 \delta \alpha_n$  respectively. The direction of transmission is given by,

$$\hat{u} = \cos \theta_t \sin \phi_t \hat{x} + \sin \theta_t \sin \phi_t \hat{y} + \cos \theta_t \hat{z} \quad (5)$$

The distance vector from the  $n^{\text{th}}$  element to the observation point P is denoted by  $\vec{r}_n$  which can be expressed as,

$$\vec{r}_n = \vec{r}_0 - \vec{r}'_{ng} \quad (6)$$

$\vec{r}_0$  is the position vector of the observation point P, while  $\vec{r}'_{ng}$  is the position vector of the  $n^{\text{th}}$  element with respect to the origin of the Cartesian coordinate system and can be expressed as,

$$\vec{r}'_{ng} = \vec{r}_c + \vec{r}'_{nl} \quad (7)$$

where

$$\vec{r}_c = x_c \hat{x} + y_c \hat{y} + z_c \hat{z} \quad (8)$$

and  $\vec{r}'_{nl}$  is the position vector of the  $n^{\text{th}}$  element with respect to the local coordinate system  $\hat{n} = \hat{t} \times \hat{v}$  with origin at the center of the array. In terms of their scalar components along the Cartesian unit vectors, the unit vectors along the t, v and n-axis are  $\hat{t} = t_x \hat{x} + t_y \hat{y} + t_z \hat{z}$ ,

$$\hat{v} = v_x \hat{x} + v_y \hat{y} + v_z \hat{z}, \text{ and}$$

$$\hat{n} = n_x \hat{x} + n_y \hat{y} + n_z \hat{z}, \text{ respectively.}$$

Using the equations described above, and making the usual far-field approximations, equation (2) becomes,

$$F_N(\theta, \phi) = \sum_{n=1}^N |I'_n| e^{j(\alpha_n + \delta \alpha_n)} e^{j\beta (x'_n \sin \theta_t \cos \phi_t + y'_n \sin \theta_t \sin \phi_t + z'_n \cos \theta_t)} \quad (9)$$

$$\text{Where, } |I'_n| = (1 + \delta I_n) |I_n|, \quad (10)$$

$$x'_n = x_c + \left(-\frac{L}{2} + (n-1)d_t\right) t_x + \delta_t t_x + \delta_v v_x + f(t) n_x \quad (11)$$

$$y'_n = y_c + \left(-\frac{L}{2} + (n-1)d_t\right) t_y + \delta_t t_y + \delta_v v_y + f(t) n_y \quad (12)$$

$$z'_n = z_c + \left(-\frac{L}{2} + (n-1)d_t\right) t_z + \delta_t t_z + \delta_v v_z + f(t) n_z \quad (13)$$

In equations (11) to (13),  $L_t$  is the length of the linear array along the t-axis. In arriving at these equations, it was assumed that the location of the elements is a random variable with independent distributions along the transversal and vertical directions. Both distributions are assumed to be normal with mean equal to the "real" location of the elements and with a respective standard deviation  $\sigma_{\delta_t}$  and  $\sigma_{\delta_v}$ . The  $\delta_t$  and  $\delta_v$  represent samples of such distributions. In the code,  $\sigma_{\delta_t}$  and  $\sigma_{\delta_v}$  are specified as inputs.  $f(t)$  is the flexing of the array aperture along the t-axis. Here, it is assumed that  $f(t)$  varies linearly from the center to the edge of the array. The slope of this variation is also an input to the code.

### I- Beam Scanning:

Two different options for beam scanning were incorporated into this simulation. These are phase scanning and true-time delay scanning. These may be used for scanning the main beam of the field radiated by either the individual panels as well as that of the array of panels. Both options are discussed presently.

#### a) Phase Scanning:

By prescribing the elements with a progressive phase shift given by,

$$\alpha_n = \beta_t = \beta \hat{u}_0 \cdot \vec{r}'_{ng} \quad (14)$$

it is possible to point the main beam in a given direction, say  $\hat{u}_0$ . Equation (9) can be written now as,

$$F_N(\theta, \phi) = \sum_{n=1}^N |I'_n| e^{j\delta \alpha_n} e^{j(\beta \hat{u}_0 \cdot \vec{r}'_{ng} + \beta_t)} \quad (15)$$

The above expression produces a maximum radiation in a direction given by,

$$\hat{u}_0 = \sin \theta_0 \cos \phi_0 \hat{x} + \sin \theta_0 \sin \phi_0 \hat{y} + \cos \theta_0 \hat{z} \quad (16)$$

#### b) True Time-Delay Scanning:

The following description is a generalization of the description found in Wille et. al. [3]. In the true time-delay method, the progressive phase-shift is achieved by using N-bit "time-shifters" as opposed

to phase shifters. For the  $n^{\text{th}}$  element, this is achieved by propagating the excitation of the element through a delay line whose length is designed to provide a time delay given by,

$$t_n(\theta_0, \phi_0) = \frac{(\hat{u}_0 \cdot \vec{r}'_{ng})}{c} \quad (17)$$

where  $c$  = speed of light in free-space. For all frequencies  $\omega = 2\pi f$ , where  $f$  is the frequency of the excitation in Hertz, the phase of the excitation is now given by,

$$\beta_i = -\omega t_n(\theta_0, \phi_0) \quad (18)$$

Substituting equation (18) into equation (15), we obtain,

$$F_N(\theta, \phi) = \sum_{n=1}^N |I'_n| e^{j(\beta \hat{u} \cdot \vec{r}'_{ng} - \omega t_n(\theta_0, \phi_0))} \quad (19)$$

which also produces a maximum radiation in the direction  $\theta_0, \phi_0$ . In this case, however, the time-delay factor is independent of frequency.

### c) Phase/Time-Delay Quantization Error:

The quantized phase/time-delay factor results from the use of N-bits phase/time-delay shifters. The number of bits N, is an input to the computer program. Due to the quantization process, the actual phase/time-delay factor realized may not be exactly equal to the specified value. The resulting quantization error may be expressed as:

$$\delta\beta_i = \beta_i - \bar{\beta}_i \quad (20)$$

where  $\delta\beta_i$  is the error,  $\beta_i$  is the specified phase/time-delay factor as given by either equation (14) or equation (18), and  $\bar{\beta}_i$  is the quantized phase time/delay shift factor. Note that  $\delta\beta_i$  can be either positive or negative depending on whether  $\bar{\beta}_i$  is smaller or larger than  $\beta_i$ . Considering the phase/time-delay quantizing error, equation (9) becomes,

$$F_N(\theta, \phi) = \sum_{n=1}^N |I'_n| e^{j\delta\alpha_n} e^{j[\beta(x'_n \sin \theta, \cos \phi_i + y'_n \sin \theta, \sin \phi_i + \cos \theta_i) + \bar{\beta}_i]} \quad (21)$$

## 2- Pattern Synthesis:

It is often of interest to achieve a narrow main beam, accompanied by a low side lobe level. One of the most important methods is the Taylor Line-Source Design Method [4]. Taylor perfected this method for continuous line source antennas. Various authors, including Villeneuve [5] have developed several approaches of applying Taylor's

method to arrays of discrete elements. Villeneuve showed that for discrete, uniformly spaced arrays, exciting the array elements with samples of the continuous distribution produces little differences in the excitations. Thus, the pattern realized by exciting the elements with samples of the continuous distribution, is undistinguishable from the pattern realized by exciting the elements with the corresponding distribution for discrete arrays. The agreement improves for larger arrays. Here we use the sampling method to compute the excitation of the elements.

## B- ARRAY PANELS

In this section, the pattern of a planar N by M elements array is discussed. The planar array is shown in Figure 2. Such array may be constructed by aligning M linear arrays- of the type described in section II-A - along the v-axis. The spacing between the M linear arrays along the v-axis is  $d_v$ . Recalling the principle of pattern multiplication, the field pattern of the planar array can be expressed as,

$$F_{NM} = e_M(\theta, \phi) f_M(\theta, \phi) \quad (22)$$

In this case, the element pattern is the field pattern of a linear array given by equation (1) and re-stated here as:

$$e_M(\theta, \phi) = e_N^*(\theta, \phi) f_N(\theta, \phi) \quad (23)$$

Thus,

$$F_{NM} = e_N^*(\theta, \phi) f_N(\theta, \phi) f_M(\theta, \phi) \quad (24)$$

where  $f_N(\theta, \phi)$  is given by equation (2) (for isotropic elements) and

$$f_M(\theta, \phi) = \sum_{m=1}^M |I'_m| e^{j\delta\alpha_m} e^{j\beta(x'_m \sin \theta, \cos \phi_i + y'_m \sin \theta, \sin \phi_i + z'_m \cos \theta_i) + \bar{\beta}_i} \quad (25)$$

In equation (25),  $|I'_m|$  is the magnitude of the excitation current with error at the  $n^{\text{th}}$  element given by,

$$|I'_m| = (1 + \delta I_m) |I_m| \quad (26)$$

where  $|I_m|$  is the magnitude of the non-error excitation and  $\delta I_m$  are samples of a normal distribution with zero mean and variance  $\sigma_{\delta I_m}^2$ . Also,  $\delta\alpha_m$  is the random error in the phase of the

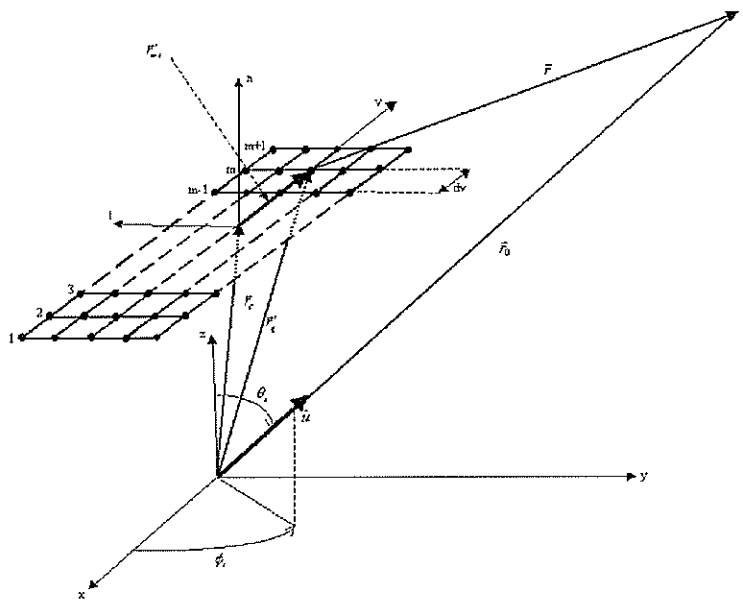


Figure 2:  $N$  by  $M$  Elements Planar Array

excitation. Here,  $\bar{\beta}_v$  is the quantized phase/time-delay factor, which can be computed in a manner similar to the one described in section II-A-1. The phases  $\bar{\beta}_t$  and  $\bar{\beta}_v$  are independent, but usually adjusted so that the main beam is directed in the same direction. Finally,

$$x'_m = x_c + \left( -\frac{L_v}{2} + (m-1)d_v \right) v_x + \delta_t t_x + \delta_v v_x + f(v)n_x \quad (27)$$

$$y'_m = y_c + \left( -\frac{L_v}{2} + (m-1)d_v \right) v_y + \delta_t t_y + \delta_v v_y + f(v)n_y \quad (28)$$

$$z'_m = z_c + \left( -\frac{L_v}{2} + (m-1)d_v \right) v_z + \delta_t t_z + \delta_v v_z + f(v)n_z \quad (29)$$

$L_v$  is the length of the array along the  $v$ -axis and  $f(v)$  is the flexing of the array aperture along the  $v$ -axis. It is assumed that  $f(v)$  varies linearly. The remaining variables were defined in previous sections. We can consider elements which are not isotropic in which case  $e(\theta, \phi)$  is directive. Included in the code are three different options for the element pattern. These are isotropic, cosine squared and cardioid element patterns.

### C- ARRAY OF PANELS

The procedure described in section II-B can be used to compute the pattern of an array of  $N$  by  $M$  panels. In this case, the individual array elements shown as dots in Figure 2 are panels. The element

pattern of the array of panels is the field pattern of a reference panel. The pattern of a panel may be computed using the procedure described in section II-B also. This can be expressed simply as,

$$F'_{NM} = e'_N(\theta, \phi) F_{NM}(\theta, \phi) \quad (30)$$

where  $F'_{NM}$  is the field of the array of panels,  $e'_N(\theta, \phi)$  is the element pattern of a reference panel given by equation (25) and  $F_{NM}(\theta, \phi)$  is the array factor of the array of panels which can also be computed as in equation (25). These ideas were used here to write a code capable of computing the field-pattern of an  $N$  by  $M$  panels antenna array.

### III- RESULTS

The purpose of this section is twofold. First, it serves as a validation of the results obtained with the code described here. Second, it serves as an implicit demonstration of the potential of the code. For the sake of completeness, patterns for linear arrays, array panels and, an array of panels are included here. Some results for directivity, gain and sidelobe level are also included. All patterns are computed at increments of half a degree in elevation and a degree in azimuth to insure convergence. The linear arrays are oriented along the  $x$ -axis so that the  $t$ -axis coincides with the  $x$ -axis. The array panels are oriented in the  $x$ - $y$  plane so that the  $t$ -axis and the  $v$ -axis coincide with the  $x$ -

axis and y-axis, respectively. All patterns are computed in the x-z plane. The random-error patterns shown here were computed using the following data: RMS amplitude error = 0.002 units. RMS phase error = 10.00 degrees, RMS error in the elements location in both x and y directions = 0.002 cm, and RMS error in element pattern = 0.0. Unless stated otherwise, the element spacing is 0.5 cm, which corresponds to a  $\frac{\lambda}{2}$  element spacing at 30 GHz. These values were chosen accordingly to examples found in the literature [6].

### A- LINEAR ARRAYS

Patterns shown in Figure 3 correspond to the normalized field-pattern of a 20-elements linear array. Two graphs are shown in Figure 3. The solid line corresponds to the normalized pattern of the array with uniform illumination. Experience as well as results found in the literature, validate the field pattern of this uniformly excited array. For instance, the directivity, gain, and sidelobe level were computed for this array also with the code described here. The directivity is 10, the gain 10 dB, and the sidelobe level -13.3 dB. These quantities further validate the results. The dotted line corresponds to a Taylor synthesized pattern with -25 dB sidelobe level ( $\bar{n} = 5$ ). The Taylor weightings were validated with results found in the literature [4]. The gain, directivity, and sidelobe level for this case array are 9.10, 9.59 dB and -25.1 dB as expected. Figure 4 shows the pattern for the same 20-elements Taylor synthesized array scanned to 45°. In this figure, the solid line represents the non-error while the dotted line corresponds to the error-pattern. In computing this pattern, only random errors were considered.

### B- ARRAY PANELS

In this section, a number of no-random-error as well as random-error- patterns are shown. The error-patterns are validated against examples found in the literature [6]. However, these examples correspond to average patterns in a statistical sense. Meanwhile, the patterns shown here are computed considering actual random variations. The validation process consists of confirming various trends in tolerance analysis reported in the literature [6]. For a given set of tolerances, these trends are: 1- the rise in sidelobe level due to random error increases as design sidelobe level decreases; 2- the pattern deterioration decreases as the array is enlarged; 3- the sidelobe level increase due to random error does not depend on scan angle;

4- pattern deterioration is larger for an L elements linear array than for an L X L elements array; and 5- the pattern deterioration is mostly a result of translational errors in the position of the elements. A number of patterns were plotted to examine these trends. These are shown in figures 5 to 9. In these figures, the non-error patterns are plotted with a solid line while the error-patterns are plotted with a dotted line.

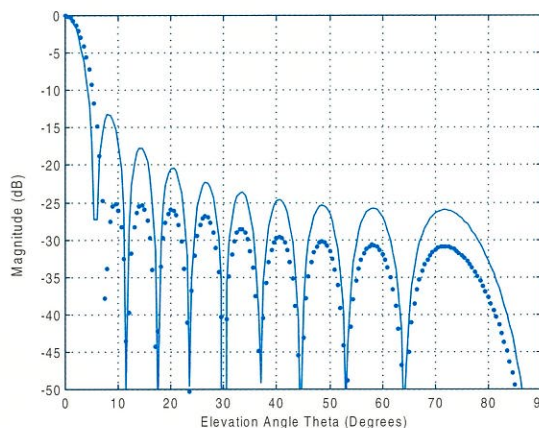


Figure 3: Pattern for a 20-elements linear array with uniform illumination (solid), -25 dB design sidelobe level (dotted)

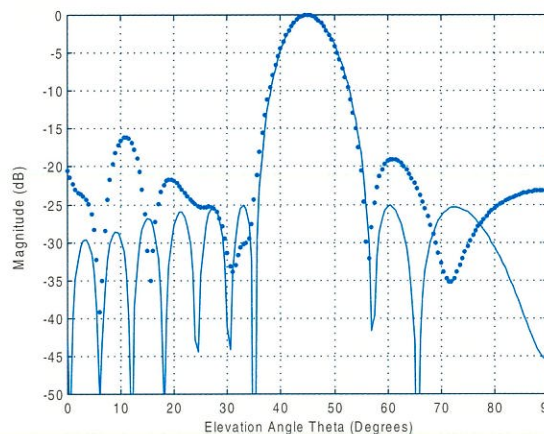
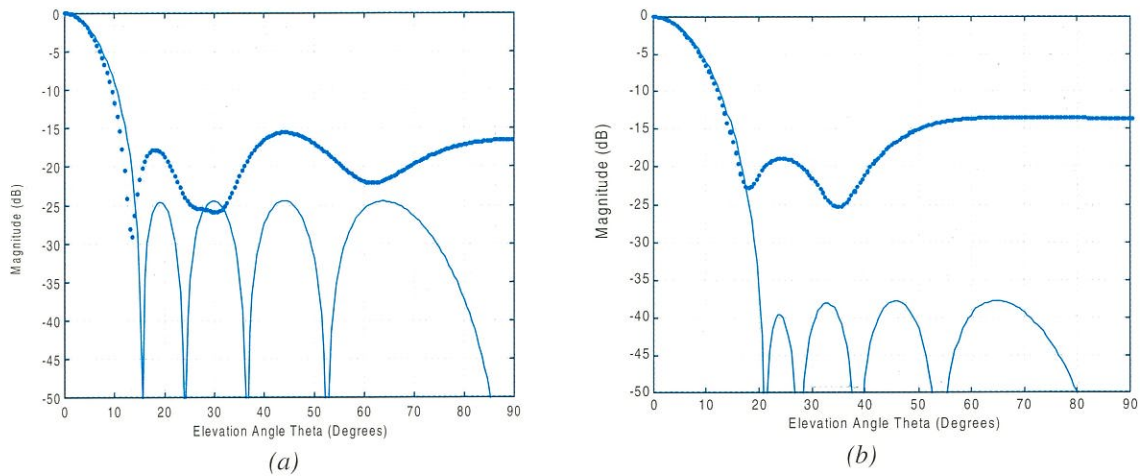


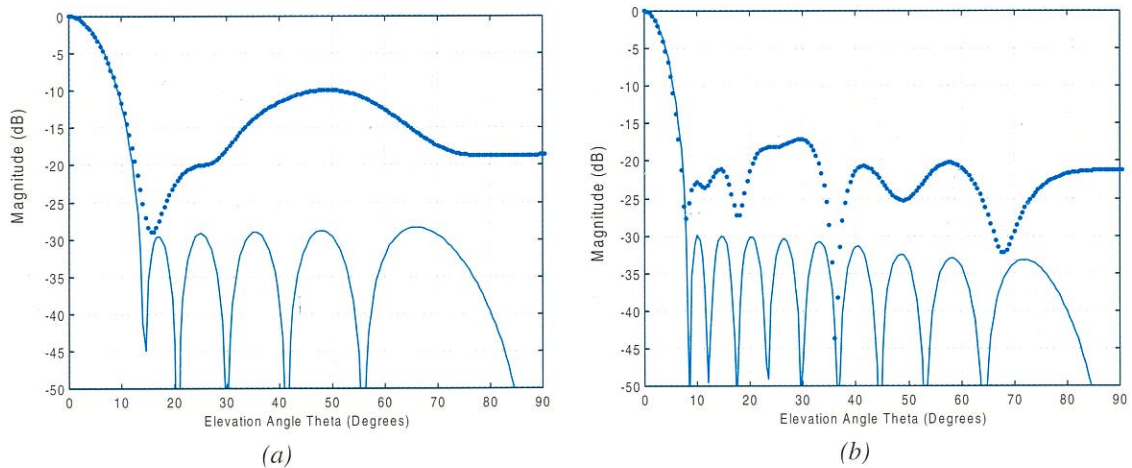
Figure 4: Pattern for a scanned 20-elements linear array with uniform illumination (solid), -25 dB design sidelobe level (dotted)

Figure 5 (a) shows the pattern for a 10 X 10 elements planar array with -25 dB design sidelobe level ( $\bar{n} = 5$ ), while Figure 5 (b) shows the pattern for the same planar array but with a -40 dB ( $\bar{n} = 10$ ) design sidelobe level. The rise in the sidelobe level is readily noticed, thus confirming the first trend.

The second trend may be examined through Figure 6. Figure 6 (a) shows the pattern for a 12 X



**Figure 5:** Error (dotted) vs. Non-error (solid) Pattern for 10 by 10 elements planar array with (a)  $-25$  dB Taylor Distribution (b)  $-40$  dB Taylor Distribution



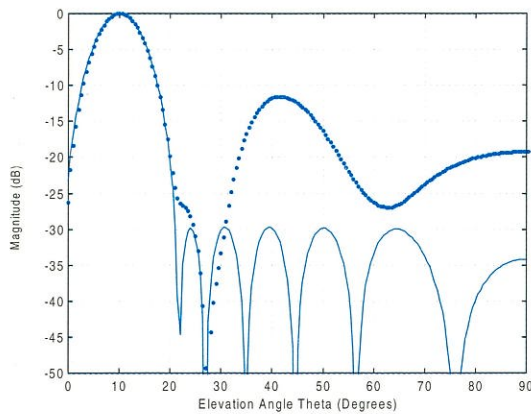
**Figure 6:** Error (dotted) vs. Non-error (solid) pattern for a (a) 12 by 12 elements array (b) 20 by 20 elements array with  $-30$  dB Taylor Distribution

12 elements array, while Figure 6 (b) shows the pattern for a 20 X 20 elements array. Both arrays have a  $-30$  dB ( $\bar{n}=7$ ) Taylor distribution. It is obvious that the rise in the sidelobe level is smaller for the larger array.

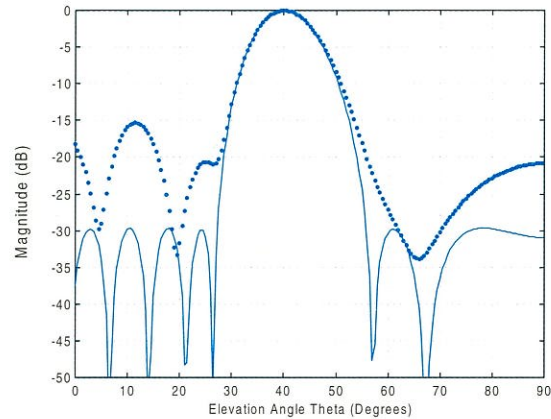
Figure 7 considers the third trend. In this case, the pattern of two 15 X 15 elements arrays are shown. Each array has a  $-25$  dB ( $\bar{n}=5$ ) Taylor distribution. A close look at the figure might suggest that in the average the sidelobe level variation be about the same in both cases. To examine the fourth trend, we consider Figure 2 and Figure 8. Figure 2 shows the error vs. non-error pattern for a 20 elements linear array with a  $-25$  dB ( $\bar{n}=5$ ) Taylor distribution, while Figure 8 shows the error vs. non-error pattern for a 20X20 elements

array with the same illumination. Examination of the two figures confirms the trend. Finally, in Figure 9, the error pattern considering translational errors only and the error pattern considering excitation errors only are both plotted vs. the non-error pattern. The array considered here is a 10 X 10 elements array with a  $-25$  dB ( $\bar{n}=5$ ) Taylor Distribution. The solid line corresponds to the non-error pattern while the dotted line corresponds to the translational errors only pattern. The dashed line corresponds to the excitation errors only pattern. This plot superimposes precisely over the no error pattern, thus confirming the fifth trend.

For completeness, this section is concluded with Figure 10 showing the “systematic-error-pattern” vs. non-error of a 20 X 20 elements array



(a)



(b)

**Figure 7:** Error (dotted) vs. Non-error (solid) pattern for a 15X15 elements array scanned (a) scanned 10 degrees (b) 40 degrees from broadside

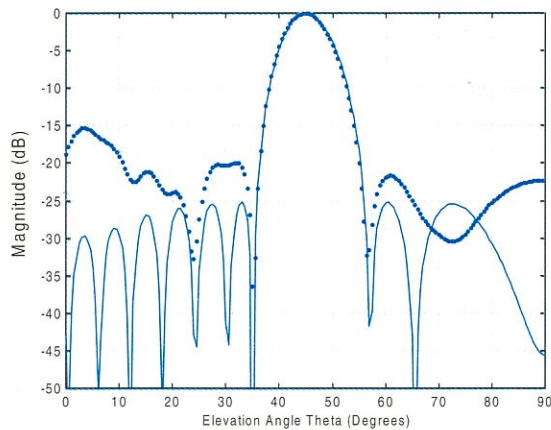


**Figure 8:** Error (dotted) vs. Non-error (solid) pattern for 20X20 planar array

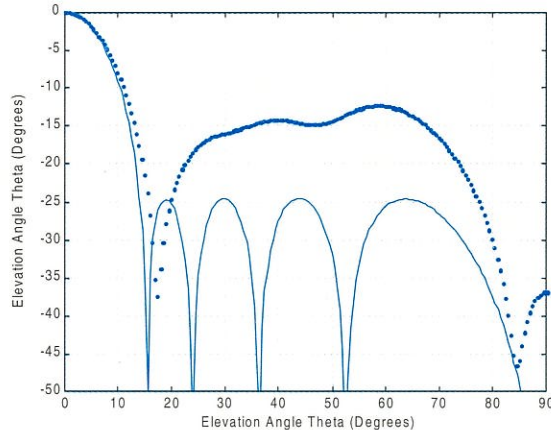


**Figure 9:** Error (dotted/dashed) vs. Non-error pattern for 10X10 planar array

with  $-25$  dB Taylor distribution. The systematic errors considered here are the flexing of the face of the array and N-bit quantization phase/time-delay shift error. The flexing of the array is assumed to vary linearly from the center to the edge of the array. In the results shown in Figure 10, the slope of the linear variation was chosen so that the maximum flexing would be 0.002 cm. Also, 3-bit phase-shifters are used to steer the main beam. It appears as if systematic errors had a slightly less impact on the array pattern than random errors.

### C- ARRAY OF PANELS

In this case, we consider the field pattern of an array of panels. The specific array considered here is based on the low-altitude space-based radar

(LASBR) described in the literature [7]. The LASBR is a 13.8m X 63.3m planar array. It consists of 49,152 elements distributed over 32 array panels. The specific arrangement of the panels as well as that of the elements within a panel is unknown. The gain for LASBR is 53 dB. It operates at a center frequency of 1.275 GHz. The array of panels considered here is a 13.1m X 63.3m array. It consists of 48,960 elements distributed over 32 panels. The panels are arranged in an array of 4 X 32 panels, with 90 X 17 elements per panel. The gain for this array is 38.8 dB. It is considerably lower than the LASBR, but these two arrays are not exactly the same. The array considered here also operates at 1.275 GHz. Figure 11 (a) shows the non-error pattern for this array, while Figure 11 (b) shows the random-error-pattern for this array. The

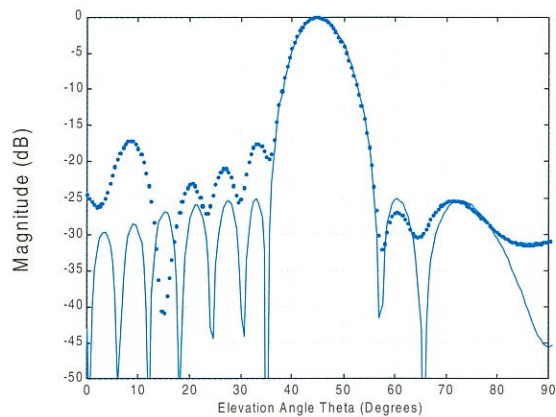


**Figure 10:** Systematic-Errors vs. Non-error Pattern for a 20 X 20 elements array

patterns are computed in the  $y$ - $z$  plane. A considerable increase in sidelobe level may be observed in the error case. The RMS error in element location is 2mm, which may account for the considerably large increase in sidelobe level.

#### IV- CONCLUDING REMARKS

A computer simulation to determine the field-pattern of arbitrarily oriented very large phase/time delay scanned antennas was developed. The simulation takes into account errors present in antenna arrays. These are systematic and random errors. The systematic errors considered here are the finite quantization of the phase produced by the use of digital N-bits phase/time-delay shifters and the flexing of the array aperture due to its large size and weight. The random errors considered are

those caused by variations on the amplitude and phase of the elements current, variations on the radiation pattern of the elements, and missing elements (due to catastrophic failure), and variations in the location of the elements. To validate the simulation a number of patterns were computed. These included patterns of linear arrays, array panels, and arrays of panels. Experience as well as specific examples validated the ideal patterns. The “random-error-patterns” were compared to specific trends noted in earlier studies. The behavior of the computed patterns confirmed such trends.

A simulation like this is a useful tool for assessing the effect of tolerances on the performance of an antenna array. It can also be used as a design tool to determine required design parameters necessary to achieve a desired sidelobe

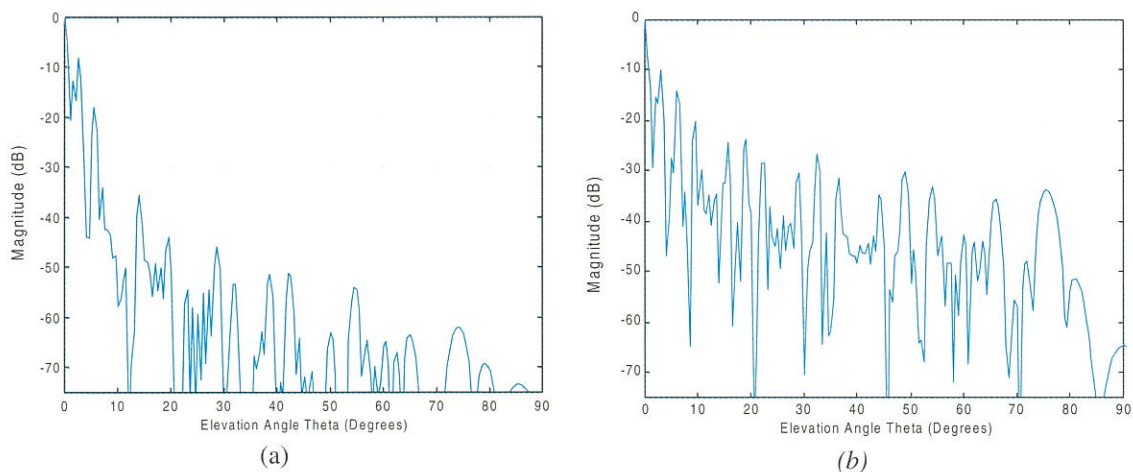


**Figure 11:** (a) Non-error Pattern (b) Error Pattern for a 4X32 panel array

level. There are some areas where the code could be improved. For instance, other types of element patterns could be considered. Moreover, the simulation could be modified to accept measured element patterns data.

#### V- ACKNOWLEDGEMENTS

The author wishes to thank Dr. Krishna Pasala for many helpful discussions. The support and interest of Dr. Stephen W. Schneider is acknowledged. Mr. John Mehr and Mr. Jim Mudd offered many helpful suggestions. The constant help received from Ms. Donna Gurnick at the AFIT Library is greatly appreciated.

The work published here was done under the auspices of the Air Force Office of Scientific Research (AFOSR) as part of the 1998 Summer Faculty Research Program.

#### VI- REFERENCES

- 1- Collin, R.E., and Zucker, F.J. "Antenna Theory Part 1," McGraw-Hill , NY, 1969
- 2- Allen J. L. et.al. "Phased Array Antenna Studies: Tech Report NO. 236, 1 July 60 – 1 July 61, Lexington MA, Massachusetts Institute of Technology, Lincoln Labs, 13 Nov 1961.
- 3- Wille Ng, et.al. "The First Demonstration of an Optically Steered Microwave Phased Array Antenna Using True-Time-Delay," *Jou. Lighth. Tech.*, Vol.9.NO.9, Sep.1991.
- 4- Taylor, T.T. "Design of Line-Source Antennas for Narrow Beamwidth and Low Sidelobes," *I.R.E. Transactions on Antennas and Propagation*, AP-3. NO. 1: 16-28, January 1955.
- 5- Villaneuve, A.T. "Taylor Patterns for Discrete Arrays," *IEEE Trans. on Antennas and Propagations*, AP-32: 1089-1093, October 1984.
- 6- Chrisman, B.P. "Planar Array Antenna Design Analysis Volume I," MS Thesis, Air Force Institute of Technology, Wright-Patterson AFB, Dayton, OH, Dec 1989 (AD-A215 537).
- 7- Cantafio, L. J. *Spaced-Based Radar*, Artech House, 1989.